Made available through Montana State University's ScholarWorks

Combining Wide-field Imaging and Reflectance Confocal Microscopy in a Single Handheld Device

Nathaniel J. Smith; Justin Wigle; Joseph Aist; Kivanc Kose; Gary Peterson; Gary Blough; Zachary Baltzer; Paul Hemmer; William Fox; Milind Rajadhyaksha; David L. Dickensheets

Accessibility Disclaimer:

For a more accessible version of this document, please submit an accessibility request form through the Montana State University Library website.

Combining Wide-field Imaging and Reflectance Confocal Microscopy in a Single Handheld Device

Nathaniel J. Smith[1], Justin Wigle[1], Joseph Aist[1], Kivanc Kose[2], Gary Peterson[2], Gary Blough[4], Zachary Baltzer[3], Paul Hemmer[3], William Fox[3], Milind Rajadhyaksha[2], David L. Dickensheets*[1]

[1] Electrical and Computer Engineering Department, Montana State University, 611 Cobleigh Hall, Bozeman, MT, USA 59715
[2] Dermatology service, Department of Medicine, Memorial Sloan Kettering Cancer Center, 300 East 66th Street, New York, NY 10065
[3] Caliber Imaging & Diagnostics, 50 Methodist Hill Dr. #1000, Rochester, NY 14623
[4]Photon Gear, Inc., 245 David Parkway, Ontario, NY 14519

Abstract

Reflectance Confocal Microscopy (RCM) imaging shows cellular-level morphology of skin in vivo, noninvasively detecting skin lesions with high sensitivity (80-95%) and specificity (70-90%) that is 2-3X higher than that of dermoscopy. The higher specificity helps reduce false positives in dermoscopically indeterminate lesions and thus reduces biopsies of benign skin lesions by 50-70%. RCM imaging is advancing into routine use at the bedside to guide patient care in clinical settings worldwide. However, a significant challenge faced by clinicians when performing RCM imaging is knowing unambiguously the location of the small RCM field-of-view (FOV) within the context of a larger lesion. The objective lens, which has a large numerical aperture (NA) and very short working distance, obscures the skin surface surrounding the location of RCM imaging. This problem can be addressed by combining a wide-field (WF) surface imaging approach with RCM imaging within a single device. We demonstrate feasibility of WF surface imaging combined with RCM imaging by integrating a micro-camera within the objective lens of a handheld confocal microscope. We report a novel objective lens design that introduces an air gap before the final hemisphere lens element, creating space for a small WF micro-camera. The micro-camera provides long depth of field and wide FOV and is integrated inside the objective lens without significantly increasing its size or decreasing optical sectioning and resolution of RCM imaging. Preliminary clinical testing on human volunteer subjects demonstrates the new handheld microscope's ability to display a WF view surrounding the location of RCM imaging on melanocytic and non-melanocytic skin lesions.

Keywords: Reflectance Confocal Microscopy RCM, Wide-field integration with RCM, wide-field imaging, micro-camera inside a microscope objective

*davidd@ece.montana.edu; phone 1 406 994-7874;

Photonics in Dermatology and Plastic Surgery 2025, edited by Haishan Zeng, Milind Rajadhyaksha,
Proc. of SPIE Vol. 13292, 1329203 · © 2025 SPIE · 1605-7422
doi: 10.1117/12.3040558

1. INTRODUCTION AND BACKGROUND

Clinical reflectance confocal microscopy (RCM) imaging for *in vivo* analysis of skin lesions at the cellular level is becoming a more widely utilized diagnostic tool for use at the bedside, saving hours or days waiting for conventional pathology results, and with similar overall sensitivity (80-95%) and specificity (70-90%) in detecting skin malignancies non-invasively.[1][2] However, the RCM objective lens with its large NA (~0.9) and short working distance has a significant contact area with the skin (diameter ~10 mm), obscuring the region of interest on the skin where RCM imaging (field-of-view ~0.75mm) is being done.[3] Consequently, during examination the clinician is uncertain precisely where, within a lesion, subsurface RCM imaging is occurring.

The goal of this project is to provide concurrent wide-field (WF) surface imaging of the skin during RCM examination, with WF providing contextual clues for RCM image selection and interpretation. To accomplish this, one might consider using a macroscopic wide-field camera and a beam splitter to merge the image fields for the camera and the RCM instrument. Working in the space between the objective and skin was found to be impractical since the RCM NA is too large and working distance too small to allow for a beam splitter between the RCM objective lens and the skin. On the other hand, placing a beam splitter after the RCM objective lens with the WF camera imaging through the full RCM objective was found to have an insufficient field-of-view (FOV) due to vignetting within the RCM objective lens. The proposed solution, which achieves a usefully large WF FOV without adding significantly to the bulk of the optics, is to integrate a micro-camera *within the objective lens*. In this paper we report our progress and show feasibility of using a handheld confocal microscope (Vivascope 3000, Caliber I.D., Rochester, NY) with a custom RCM objective lens with integrated WF micro-camera to simultaneously show contextual surface features while maintaining the optical performance of RCM required for disease diagnosis.

We first reported this approach in 2016,[4] with a proof-of-concept demonstration on the benchtop. That demonstration used a mm-scale lensless CMOS sensor (Naneye2D-RGB) with a custom-built microlens as the WF camera. The camera was aligned and fixed at the apex of a hyper-hemisphere which was the first element of an RCM objective lens mock-up. The illumination for WF imaging was achieved using a flexible printed circuit board (PCB) with four white LEDs in contact with the hyper-hemisphere. This early-stage proof-of-concept encouraged the development of improvements we report here.

In this paper we describe the first clinical prototype instrument for concurrent RCM imaging with WF guidance. The development includes a novel RCM objective lens that maintains a high NA (~0.9) and introduces an extended air gap before the final hemispherical lens element, creating space for a small WF camera. We then assembled a commercially available, lensed WF camera and illumination LEDs onto a printed circuit board for integration into the objective lens. The WF camera provides a long depth-of-field (DOF) and wide FOV, while RCM resolution and cross-sectioning are not degraded. We describe the instrument design and assembly, the optical performance of the WF imaging mode and show early clinical results obtained with the prototype system.

2. SYSTEM DESIGN

2.1 Design concept

During dermoscopic exams using the Vivascope 3000 handheld probe, a 1mm thick window that is part of the objective lens encasement is placed in contact with the skin as shown in the left panel of Figure 1. The objective lens is inserted into the encasement, with a thin layer of gel between the objective lens and the window. The exact thickness of the gel layer is adjustable, allowing the RCM imaging beam to be focused from the surface of the skin up to a depth of a few hundred micrometers under the skin surface. The glass window, gel layer and first lens element of the objective lens (a hemisphere lens) work together as part of a nearly aplanatic group to support diffraction-limited microscopy in the skin. The contact area between the window and skin is large relative to the size of the RCM FOV. The back lens elements of the objective lens are separated from the hemisphere lens with a gap that is large enough to accommodate a printed circuit board (PCB) supporting the WF microcamera and illumination LEDs. The wide-field camera is centrally positioned near the apex of the hemisphere, while the LEDs are located in a ring around the perimeter. This arrangement is illustrated in the right panel of Figure 1. Precise mechanical assembly of the objective ensures alignment of the RCM and WF imaging components. The 4-wire camera interface and 2-wire LED drive signal are connected via flexible cable to a custom electronic interface.

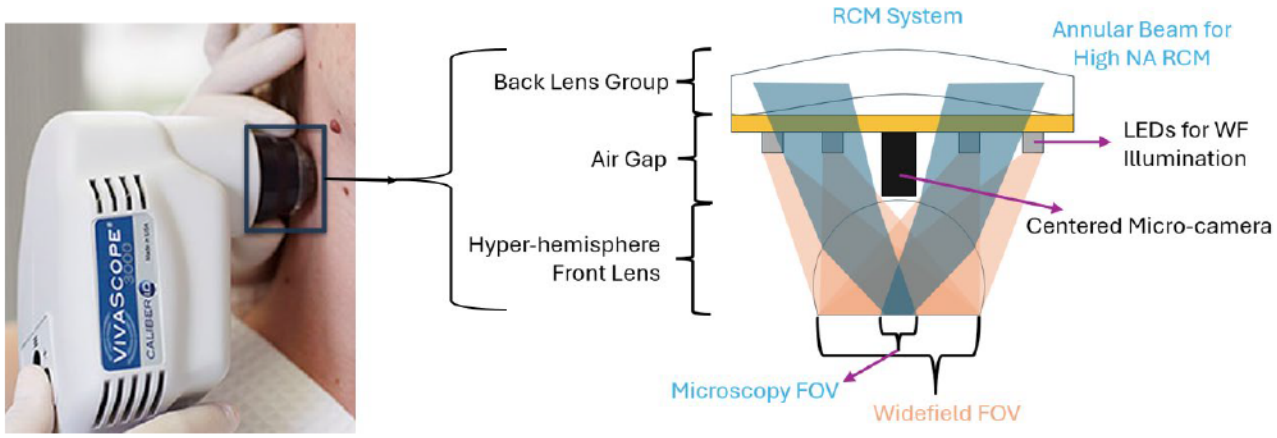


Figure 1: Vivascope 3000 handheld probe in contact with skin (left pane); Wide-field integrated RCM system showing micro-camera inserted in the air gap (right pane), with the hemisphere lens-gel-window assembly represented as a simple hyperhemisphere.

2.2 Mechanical assembly

The metal mounting for the last lens of the objective and the integrated WF circuitry is precisely machined for alignment of the optics and assembly of the flex PCB. Figure 2 (left panel) shows a view from the back side of the partially assembled objective lens holding the flexible PCB populated with LEDS and micro-camera behind the hemisphere lens. This subassembly is part of the full objective lens assembly (right panel). The objective lens is mounted to the hand-held probe and then is inserted with coupling gel into the windowed encasement which is in contact with the skin through a 1mm thick window. Note that the camera PCB introduces a central bar-shaped obscuration about 2 mm wide for the RCM beam. The impact on RCM imaging due to this obscuration appears to be minimal.



Figure 2: Mechanical assembly of objective last lens element with centered micro-camera and illuminated LEDs (left); full objective assembly before mounting onto hand-held probe (right).

2.3 Wide-field micro-camera integration

The Omnivision OV6946-RAJA Camera Cube Chip was chosen for integration inside the prototype objective lens. This camera, initially developed for endoscopy applications, fulfilled the need for a compact package that could be

integrated into our objective lens design. The physical dimension, which includes the sensor, readout electronics and multielement lens, is 1.100×1.100×2.266 mm. Power and analog readout is via a 4-terminal interface, with assembly onto the flexible printed circuit board achieved by solder-ball reflow. The sensor has 400×400 pixels, each measuring 1.75×1.75 μm. This is a color sensor with a Bayer mask overlay. The minimal 4-wire interface to the camera facilitates use of a low-profile flexible cable for transmission of the image signal to the ISP board and subsequently to a computer for display alongside the RCM microscopy image. The camera is centered, with the PCB creating a thin, bar-shaped obscuration in the optical path of the RCM scanning beam.

2.4 Illumination

Eight Inolux IN-S42ATUW white LEDs were chosen as the illumination source for WF imaging. The typical luminous intensity of this indium gallium nitride based LED is 600mcd at a forward current of 20mA over a broad spectrum between 450nm and 600nm. The physical dimension of each LED is 1.00×0.50 mm, surface mounted on the flexible printed circuit board. All eight LEDs are driven in series with a custom LED driver circuit that allows for user control over illumination brightness.

2.5 Wide-field imaging performance characterization

The datasheet for the OV6946-RAJA micro-camera specifies a focal length of 0.418mm and *f*-number of 5.0, with depth of focus from 5mm to 50mm in air. The camera is placed directly behind the 3.4mm radius hemisphere element of the RCM objective lens. Paraxial analysis predicts that the depth of focus in glass will be from 4.3mm to 8.8mm, with a best focus at approximately 5.7mm, assuming the hemisphere index of refraction is $n = 1.517$. The thickness of an aplanatic hyperhemisphere is $r(1 + 1/n)$, which for $r = 3.4$mm and $n = 1.517$ is 5.64mm, nearly coincident with the best focus depth for the micro-camera, and close to the physical thickness of the combination of hemisphere, gel and window in our setup. During RCM imaging of skin, the coupling gel thickness varies as the focal depth for RCM imaging is changed. But this change is small compared to the depth of focus for the camera which should, therefore, be operating with minimal defocus error. The paraxial magnification from sensor to skin surface is calculated to be 8.6x, yielding a field of view at the skin of approximately 6×6 mm. The measured magnification was found to be 9.5x near the center of the image, and the measured FOV was 6.5×6.5 mm. There is noticeable pincushion distortion with this camera.

The resolution of the camera is limited by diffraction, finite pixel size and de-Bayering (our image processing uses nearest-neighbor bilinear interpolation). [5] [6] [7] Considering all of those effects, the full-width at half-maximum for the line spread function (LSF) at the skin is predicted to be 37µm, and the 50% modulation frequency for the modulation transfer function (MTF) is predicted to be 10.5 mm^{-1}. Figure 3 shows the measured MTF obtained from a slanted edge measurement. The experimentally measured 50% modulation frequency is 10 mm^{-1}, close to the predicted value. The theoretically predicted MTF curve is plotted for comparison. From this result it appears that the micro-camera is performing as predicted, based on paraxial analysis and consideration of diffraction effects along with finite pixel size and interpolation.

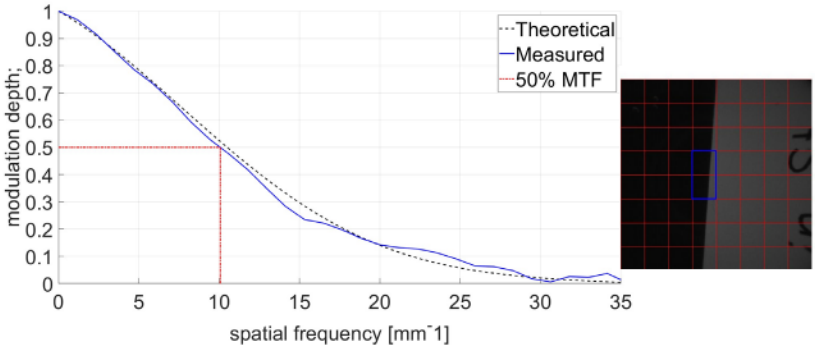


Figure 3: Widefield camera MTF measured from a slanted edge target (solid blue line). Theoretically predicted MTF is plotted for comparison (dashed black line). A representative slanted edge image is shown in the inset.

3. RESULTS

3.1 Preliminary clinical tests

Under an IRB-approved protocol, we tested our handheld microscope with the integrated WF micro-camera for RCM imaging of skin lesions in vivo on 28 volunteers. Figure 4 shows an example case, displaying the WF color image of a pigmented lesion on the forearm of a volunteer, with the corresponding RCM image. The fields of view display 6mm x 6mm area on the skin surface (WF image) and 750μm×750μm (RCM image). While moving the microscope around on the lesion, simultaneous videos of WF and RCM images are acquired. The WF image shows globular and dendritic patterns of pigmentation. The RCM image shows rings of bright basal cells at the dermal-epidermal junction, interspersed within spinous layers in the surrounding epidermis, showing cobblestone patterns of dark nuclei within honeycomb patterns of bright cells. The sharpness and contrast of nuclear and cellular patterns in the RCM images indicates that optical sectioning and resolution with the centrally-obscured pupil is sufficiently preserved for diagnostic quality imaging.

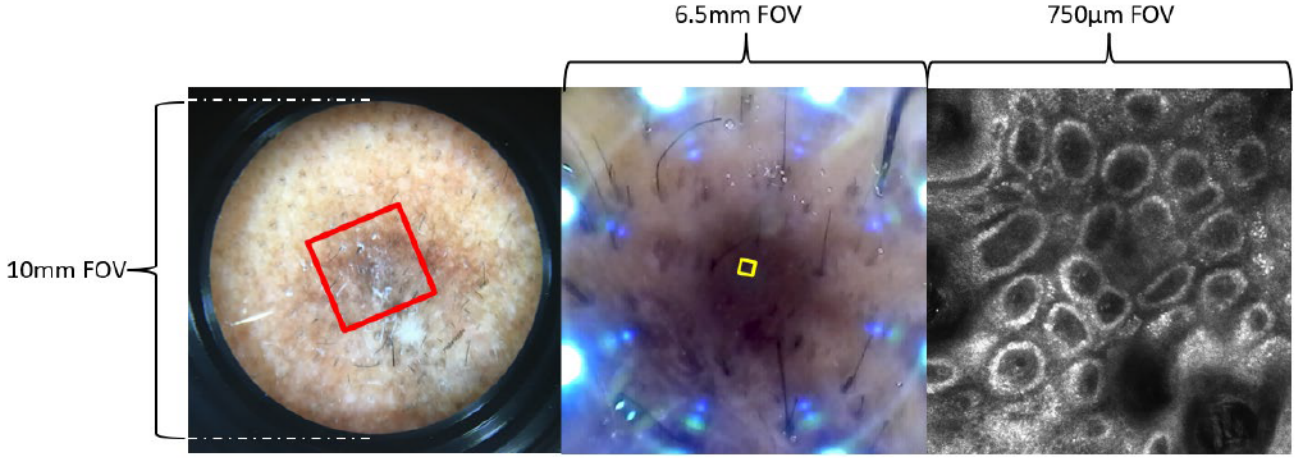
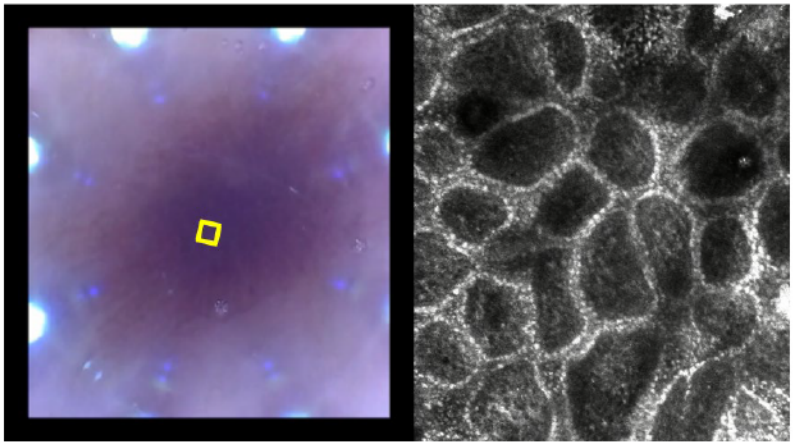


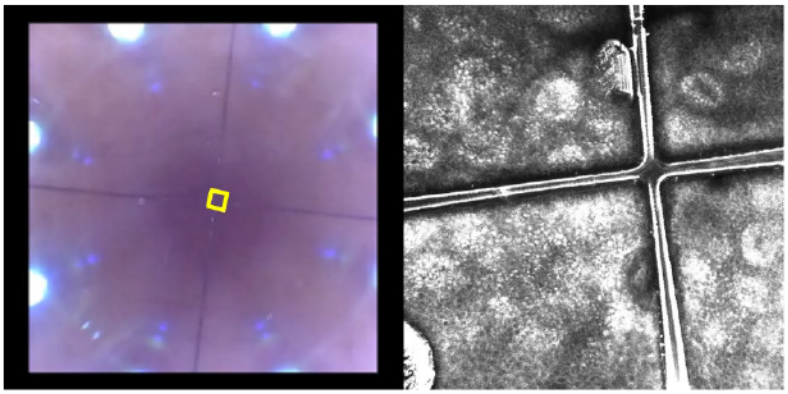
Figure 4: Three FOVs showing the (A) clinical image taken with a smartphone dermoscope, (B) WF image from the micro-camera integrated inside the objective, where the WF FOV corresponds to the red box in panel A; (C) RCM image at the location of the blue box shown in panel (B).

3.2 Simultaneous wide-field and RCM imaging

Real-time WF imaging guides the clinician while scanning the RCM FOV. The WF viewport is used to locate a region of interest within melanocytic and non-melanocytic lesions. The clinician is then able to acquire RCM image stacks required for accurate diagnosis as shown in video 1 (supplementary material). A fine wire grid overlaid on the skin serves as a fiducial to aid in our assessment of location registration between WF and RCM, as shown in video 2 (supplementary material).



Video 1: "Smith_Nate_PW_video1" Simultaneous real-time imaging of WF field of view (left pane) and RCM field of view (right pane) http://dx.doi.org/10.1117/12.3040558.1



Video 2: "Smith_Nate_PW_video2" Imaging with a wire-grid fiducial on the skin surface: WF field of view (left pane) and RCM field of view (right pane) http://dx.doi.org/10.1117/12.3040558.2

4. SUMMARY AND DISCUSSION

4.1 Key conclusions

We have demonstrated the feasibility of practical implementation of simultaneous WF surface imaging integrated with RCM in a hand-held probe for bedside dermoscopy examination by a clinician. This was achieved by integrating a micro-camera inside the objective lens of the RCM instrument. The innovative objective lens in our design maintains a high NA, ensuring the WF integration does not compromise the optical sectioning or resolution of the RCM imaging. Our improvement from the benchtop system previously published [4] shows preliminary clinical tests validating the potential for use of WF imaging to unambiguously show the location of RCM imaging within a lesion. WF imaging provides a 6mm × 6mm illuminated FOV, enabling RCM imaging of cellular morphology to be associated with surface morphology with greater precision.

Optical performance of the micro-camera integrated inside the objective, with a measured magnification of 9.5x, exhibited an MTF 50% modulation spatial frequency of 10 mm^{-1}, closely matching predicted performance This performance is sufficient for a clinician to identify surface indicators, guiding analysis with RCM for an accurate detection of disease. Our integration of WF imaging inside a hand-held confocal microscope provides the means for a clinician to unambiguously know the location of the FOV in the context of the larger lesion. Subsequent studies will investigate whether this added information increases the diagnostic utility of the probe, thus further reducing the need for unnecessary biopsies.

4.2 Future improvements

Further improvements are necessary for a clinical instrument. One area for improvement will address illumination uniformity for WF imaging. The eight LEDs in a ring create an eight-lobed illumination pattern (e.g. see Figure 4(B)). White balancing compensates for this effect but is not perfect. We are investigating other possible configurations for the LEDs in the assembly. Direct specular reflection from some of the glass surfaces can also be noticed (e.g. Figures 5 and 6) in the periphery of the WF images. We are investigating the use of crossed polarization between the LEDs and the WF camera as a way to suppress these "hot spots" in the image. Finally, the RCM laser at 830 nm wavelength is coupling weakly into the WF sensor, leading to the pinkish haze in the simultaneous WF/RCM images (Figures 5 and 6). We are investigating mitigation strategies for this effect, including a spectral filter over the camera to block the RCM wavelength, and time-interleaving for WF and RCM image acquisition. Also, we are assessing the feasibility for accurate real-time automated registration of the low-resolution image stream from the integrated WF camera to a reference high-resolution clinical dermoscopic image to potentially enhance the diagnostic utility of the contextual image. Further refinement of the registration processes may also allow future modes of use such as video-mosaicking to extend both the WF and RCM fields of view.

ACKNOWLEDGEMENTS

This work was supported by the National Institute of Health (NIH) and the National Institute of Biomedical Imaging and Bioengineering (NIBIB), grant R01EB028752. The effort at MSKCC was partly supported by Core Center grant P30CA008748. The authors gratefully acknowledge the many helpful contributions from Val Tretter and Nick George at Montana State University.

COI disclosure: Dr. Rajadhyaksha is a former employee of and owns equity in Caliber I.D., the company that manufactures and sells the VivaScope confocal microscope.

REFERENCES

[1] S. Abeytunge, Y. Li, B. Larson, G. Peterson, E. Seltzer, R. Toledo-Crow and M. Rajadhyaksha, "Confocal microscopy with strip mosaicing for rapid imaging over large areas of excised tissue," *Journal of Biomedical Optics,* vol. 18, no. 6, pp. 061227-1-13, 2013.

[2] M. Jain, S. V. Pulijal and M. Rajadhyaksha, "The bedside diagnostic accuracy of a novice reflectance confocal microscopy reader for skin cancer detection in vivo in real-time: understanding the challenges and potential pitfalls," in *SPIE BiOS*, San Francisco, 2017.

[3] D. L. Dickensheets, T. Liu, S. Kreitinger, G. Peterson and M. Rajadhyaksha, "Toward Smaller, More Useable Clinical Confocal Microscopes with Advanced Scanning and Integreated Wide-Field Guidance," in *Biophotonics Congress: Biomedical Optics Congress*, 2018.

[4] D. L. Dickensheets, S. Kreitinger, G. Peterson, M. Heger and M. Rajadhyaksha, "Wide-field imaging combined with confocal microscopy using a miniature f/5 camera integrated within a high NA objective lens," *Optics Letters,* vol. 42, no. 7, pp. 1241-1244, 2017.

[5] J. Anspach and D. L. Dickensheets, "Sequential RGB color imaging with a millimeter-scale monochrome camera with a rolling shutter," *Applied Optics,* vol. 62, no. 17, pp. 4496 - 4504, 2023.

[6] J. N. Aist, "Widefield micro-camera integrated into the objective lens of a reflectance confocal microscope for concurrent image registration," Montana State University Master's Thesis, Bozeman, 2023.

[7] P. D. Burns, "sfrmat4," Burns Digital Imaging, 2 June 2020. [Online]. Available: http://burnsdigitalimaging.com/software/sfrmat/. [Accessed 30 December 2024].

[8] D. S. Gareau, Y. Li, B. Huang, Z. Eastman, N. S. Kishwar and M. Rajadhyaksha, "Confocal mosaicing microscopy in Mohs skin excisions: feasibility of rapid surgical pathology," *Journal of Biomedical Optics,* pp. 054001-1-12, 2008.

[9] M. Rajadhyaksha, R. R. Anderson and R. H. Webb, "Video-rate confocal scanning laser microscope for imaging human tissues in vivo," *Applied Optics,* vol. 38, no. 10, pp. 2105-2115, 1999.

[10] P. J. Dwyer, C. A. DiMarzio and M. Rajadhyaksha, "Confocal theta line-scanning microscope for imaging human tissues," *Applied Optics,* vol. 46, no. 10, pp. 1843-1851, 2007.

[11] D. S. Gareau, S. Abeytunge and M. Rajadhyaksha, "Line-scanning reflectance confocal microscopy of human skin: comparision of full-pupil and divided-pupil configurations," *Optics Letters,* vol. 34, no. 20, pp. 3235-3237, 2009.

[12] P. J. Dwyer, C. A. DiMarzio, J. M. Zavisian, W. J. Fox and M. Rajadhyaksha, "Confocal reflectance theta line scanning microscope for imaging human skin in vivo," *Optics Letter,* vol. 31, no. 7, pp. 942-944, 2006.